Marine Pollution Bulletin 146 (2019) 225–235

Contents lists available at ScienceDirect

Marine Pollution Bulletin

journal homepage: www.elsevier.com/locate/marpolbul

Physiological responses of a coccolithophore to multiple environmental drivers

Peng Jin[a,b], Nana Liu[a], Kunshan Gao[a,c,*]

[a] State Key Laboratory of Marine Environmental Science (Xiamen University)/College of Ocean and Earth Sciences, Xiamen University, Xiamen 361102, China
[b] School of Environmental Science and Engineering, Guangzhou University, Guangzhou 510006, China
[c] Laboratory for Marine Ecology and Environmental Science, Qingdao National Laboratory for Marine Science and Technology, Qingdao 266071, China

ARTICLE INFO

Keywords:
Coccolithophores
Global change
Ocean acidification
Multiple drivers
Synergistical

ABSTRACT

Ocean acidification is known to affect primary producers differentially in terms of species and environmental conditions, with controversial results obtained under different experimental setups. In this work we examined the physiological performances of the coccolithophore *Gephyrocapsa oceanica* that had been acclimated to 1000 μatm CO_2 for ~400 generations, and then exposed to multiple drivers, light intensity, light fluctuating frequency, temperature and UV radiation. Here, we show that increasing light intensity resulted in higher non-photochemical quenching and the effective absorption cross-section of PSII. The effective photochemical efficiency (Fv′/Fm′) decreased with increased levels of light, which was counterbalanced by fluctuating light regimes. The greenhouse condition acts synergistically with decreasing fluctuating light frequency to increase the Fv′/Fm′ and photosynthetic carbon fixation rate. Our data suggest that the coccolithophorid would be more stressed with increased exposures to solar UV irradiances, though its photosynthetic carbon fixation could be enhanced under the greenhouse condition.

1. Introduction

The oceans are now undergoing multiple environmental changes including ocean acidification, warming, deoxygenation, increasing light and ultraviolet (UV) exposures and decreasing nutrient availability within upper mixing layers due to enhanced stratification and reduced upward transport of nutrients in open oceans (Boyd and Hutchins, 2012; Boyd et al., 2018). A major challenge for marine scientists is to identify, quantify and understand how the concurring multiple environmental drivers (MEDs) (see Boyd and Hutchins, 2012 for definitions) impact on marine ecosystems at all levels from individual genotypes to communities (Boyd and Hutchins, 2012; Brennan and Collins, 2015; Boyd and Brown, 2015). Combined effects of the factors can either be additive, where the responses to MEDs are equal to or bigger than the sum of their individual effects, or counteractive (antagonistic) (Gunderson et al., 2016). While there have been a number of studies that documented on the responses of marine organisms to key environmental drivers alone, such as temperature, CO_2, or light levels, or to the combinations of 2, little is known about physiological responses of phytoplankton to MEDs (Riebesell and Gattuso, 2015). Approaches to look into MEDs' effects can lead to a better understanding of responses of marine biota or ecological processes to the simultaneous marine environmental changes (Boyd et al., 2019).

Coccolithophores, a key group of marine primary producers that play a crucial role in ocean carbon cycles, have been suggested to be susceptible to global ocean changes (see the review by Raven and Crawfurd, 2012 and literatures therein; Meyer and Riebesell, 2015). Over the last decade, studies showed that coccolithophores respond differentially across different species and strains or different experimental setups to changes in seawater carbonate chemistry (see summaries of Meyer and Riebesell, 2015; Feng et al., 2017; Jin et al., 2017). *Emiliania huxleyi*, the most abundant coccolithophore, decreased calcification rates under elevated CO_2 concentrations (Riebesell et al., 2000; Feng et al., 2008; Gao et al., 2009). On the other hand, light intensity (Rokitta and Rost, 2012; Jin et al., 2017), temperature (De Bodt et al., 2010; Sett et al., 2014), UV radiation (Gao et al., 2009; Xu and Gao, 2015) and nutrient concentrations (Sciandra et al., 2003) have been documented to alter responses of coccolithophores to ocean acidification (OA) treatment. In addition, discrepant responses of coccolithophores to OA, even examined under comparable conditions, have been observed, which have been attributed to species- and/or strain-specific differences (Langer et al., 2006, 2009) as well as to different carbonate chemistry manipulations (Shi et al., 2009).

Along with the ongoing OA, ocean warming (IPCC, 2014),

* Corresponding author at: State Key Laboratory of Marine Environmental Science, Xiamen University, Xiamen 361102, China.
E-mail address: ksgao@xmu.edu.cn (K. Gao).

https://doi.org/10.1016/j.marpolbul.2019.06.032
Received 6 May 2019; Received in revised form 11 June 2019; Accepted 11 June 2019

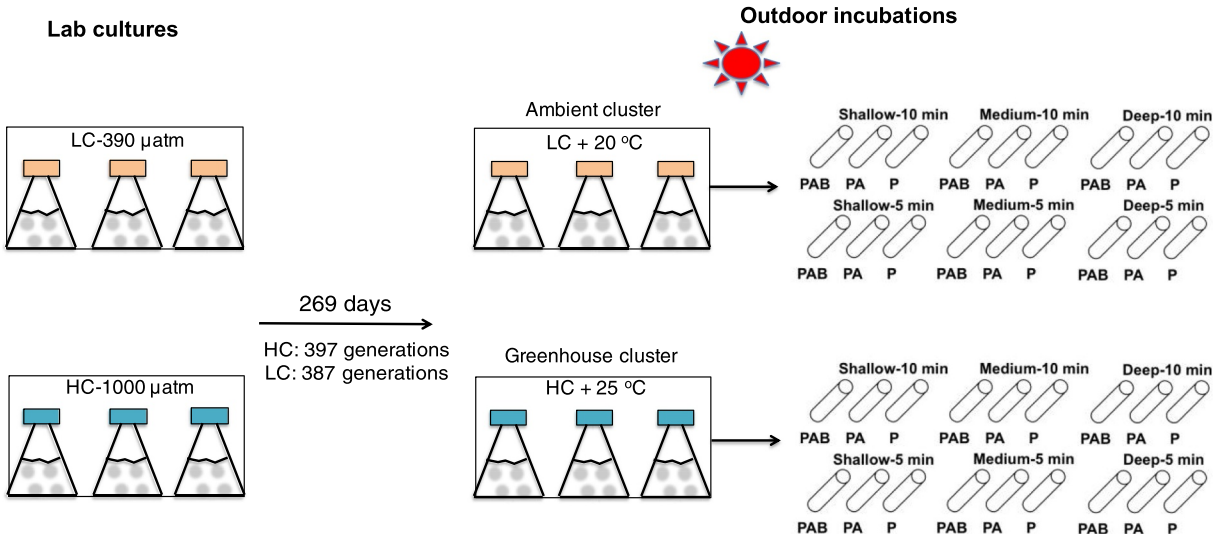

Fig. 1. Schematic overview of the experimental design of lab and outdoor incubations.

deoxygenation (Keeling et al., 2010; Schmidtko et al., 2017), shoaling of upper mixed layer (UML) (Sarmiento et al., 2004) and subsequently increasing UV exposures to the cells within this layer are supposed to compound the effects of OA (Boyd et al., 2019). Thinner UML exposes phytoplankton cells within it to higher doses of solar UV and visible radiation due to shortened mixing path within UML. Moreover, phytoplankton communities are subject to high dynamic fluctuating sunlight during the diel cycles or due to cloud covers and water movements associated with currents and winds. Each of these environmental drivers may affect cellular processes of coccolithophores both individually (light: e.g. Paasche, 1999, Zondervan, 2007; temperature: e.g. Watabe and Wilbur, 1966, Paasche, 1968) and interactively (see the reviews by Paasche, 2002, Zondervan, 2007, Raven and Crawfurd, 2012 and Gao et al., 2012 and literatures therein). For example, light density (Rokitta and Rost, 2012; Zhang et al., 2015; Jin et al., 2017), temperature (De Bodt et al., 2010; Sett et al., 2014; Milner et al., 2016), UV radiation (Gao et al., 2009; Xu and Gao, 2015) and fluctuation of light (Jin et al., 2013) could all modulate effects of OA on physiological performances of coccolithophores.

It is of general concern to explore the effects of OA under multiple drivers on marine phytoplankton and other organisms (Boyd et al., 2019), as reported previously in diatoms (CO_2 × nutrient × light × UVR, Xu et al., 2014; Li et al., 2017), however, little has been documented on this aspect in coccolithophores. Increasing levels of solar radiation can offset the impacts of elevated CO_2 on coccolithophores by compensating the increased energy costs of calcification (Rokitta and Rost, 2012; Jin et al., 2017), and these responses are also modulated by temperature (Sett et al., 2014). In addition, fluctuating light can affect energetics in phytoplankton by increasing the costs for maintenance and repair of photoinhibition, thereby potentially altering the allocation of energy to other processes (e.g. photosynthesis) (Dimier et al., 2009), and then acting with elevated CO_2 to synergistically lower photosynthetic carbon fixation by coccolithophores (Jin et al., 2013). Furthermore, energy saved from the down-regulation of CO_2-concentration mechanisms (CCMs) under elevated CO_2 conditions may benefit the recovery of UV-B-induced inhibition (Li et al., 2012; Jin et al., 2013), suggesting an antagonistic interaction between CO_2 and UV-B. Therefore, from an energetic point of view, these drivers (light intensity/light fluctuating frequency/CO_2/temperature/UVR) could act interactively to directly or indirectly affect the energy allocation of phytoplankton, and then consequently affect their physiological performances. Here, we hypothesize that OA-acclimated coccolithophores might suffer more from additional environmental stressors, and extra energy is required for the cells to sustain. To test this, we firstly clustered the variables CO_2 and temperature, and then conducted four-way factorial manipulations of CO_2&temperature and another three environmental drivers of stimulated UML depth, light fluctuating frequency and UVR to evaluate the responses of the cosmopolitan coccolithophore *Gephyrocapsa oceanica* to the multiple environmental drivers. The obtained results are intended to contribute to our knowledge of the holistic consequences of future multiple environmental changes to planktonic calcifiers.

2. Materials and methods

2.1. Culture conditions

Gephyrocapsa oceanica (NIES-1318), originally isolated from the East China Sea, was obtained from the National Institute for Environmental Studies (NIES, Japan). This strain was originally calcifying, but lost calcifying capacity before we performed the experiments as described in our previous studies (Jin et al., 2013; Jin and Gao, 2016). Three independent cultures were run semi-continuously at ambient (LC, 390 µatm) or elevated (HC, 1000 µatm) CO_2 concentrations for about 390 generations before the multiple drivers experiments were performed. To maintain stable carbonate chemistry in the cultures, initial cell concentration was 100 cells mL^{-1} and the medium was partially renewed every 6 or 7 days to restore the cell concentration to its initial level. As demonstrated in our previous study (Jin et al., 2013; Jin and Gao, 2016), such a dilution frequency and maintenance of cell concentration (exponential growth phase) can sustain the carbonate chemistry with negligible change in pH_{NBS} (< 0.06). The culture medium was prepared with artificial seawater enriched with Aquil medium (110 µM nitrate, 10 µM phosphorus; Morel et al., 1979). The cultures were maintained indoor for 269 days, corresponding to 397 generations in HC treatment and 387 generations in LC treatment, under photosynthetically active radiation (PAR) of 100 µmol photons $m^{-2} s^{-1}$ (12:12 light: dark period) in a plant growth chamber (GXZ, Ruihua, Wuhan, China) at a constant temperature of 20 °C before being transferred to the outdoor (rooftop) growth experiments under solar radiation with or without UV radiation (Fig. 1).

2.2. Outdoor experimental setup

In the outdoor incubation experiments, we used the cluster experiment approach as proposed by Boyd et al. (2010), by grouping LC and low temperature (LT, 20 °C) as "ambient cluster" and HC and high temperature (HT, 5 °C above ambient, as has been projected by the year

2100, IPCC 2013) as "greenhouse cluster" (Boyd et al., 2010) (Fig. 1). Such clustering as validated according to future CO_2 scenario is likely to be tightly coupled to simultaneous warming in most marine regimes. Three UML depths were mimicked by using 3, 5 and 7 layers of neutral density screens, in which the solar irradiance level at the bottom of the UML was 17% (shallow), 6.5% (medium) and 2% (deep) of that at sea surface, respectively. The fluctuating irradiance exposed to the cells was simulated by continually adding and removing covering layers of neutral screens, so that the cells experienced varying sunlight levels, achieving similar mixing condition as reported previously (Marra, 1978; Helbling et al., 2003). We used two different time intervals, 5 (high turnover rate of fluctuating light, HFL) and 10 min (low turnover rate of fluctuating light, LFL) to simulate the light paths from the bottom (2.0%, 6.5% or 17.0%) to the surface (100%) of UML, presenting the high light fluctuating frequency and low light fluctuating frequency, respectively. In brief, for bottom light of 2% UML, one layer of screen was removed with a 5 min interval, increasing light exposures step-wisely from 2% to 6.5%, 10%, 17%, 31%, 55% and 100%, and backward by adding the screen that decreased the light exposure from 100% to 55%, 31%, 17%, 10%, 6.5% and 2% (Fig. 2). Thus, one circulation time span (from the surface to the bottom and then back to the surface) for deep (7 layers, 2% of the surface incident PAR), medium (5 layers, 6.5% of the surface incident PAR) and shallow (3 layers, 17% of the surface incident PAR) UML depth was 80, 60 and 40 min, respectively. When the screen removal (or addition) frequency was adjusted to 10 min, one circulation for deep, medium and shallow UML depth took 160, 120 and 80 min, respectively. Despite of different turnover rates (simulated mixing rates), the total incubation durations for each stimulated UML depth was the same, 320, 240 and 160 min for shallow, medium and deep UML depth, respectively (Fig. 2). The outdoor incubation periods for shallow, medium and deep UML depth treatment were 10:30–13:10, 10:30–14:30 and 10:30–15:50 at local time, respectively (Supplementary Fig. S1).

2.3. Radiation treatments and solar irradiances measurements

Three radiation treatments were implemented: PAB, tubes covered with a 295 nm cut off filter (Ultraphan, Digefra, Munich, Germany) so that cells were exposed to PAR + Ultraviolet A (UV-A) + Ultraviolet B (UV-B), receiving irradiances above 295 nm, with a short-wavelength cut-off that excludes the lowest 15 nm of the UVB range; PA, tubes covered with Folex 320 filters, so that cells were exposed to PAR + UV-A, receiving irradiances above 320 nm; and P, tubes covered with 395 cut off foil (UV Opak, Digefra, Munich, Germany), so that the cells received irradiances above 395 nm (PAR treatment).

To initiate the outdoor cultures, laboratory stock cultures that have been grown under HC and LC conditions for ~400 generations, were transferred to 50 mL quartz tubes covered with different foils as described above at a relatively low cell density of 5×10^4 cells mL^{-1} in order to maintain stable carbonate chemistry during the incubation periods. The tubes were placed in different water baths at two constant temperatures of 20 and 25 ± 0.1 °C controlled with a circulating cooler (CTP-3000, Eyela, Tokyo, Japan). Outdoor incubations were carried out from the 9th to 23rd of October 2011. Solar PAR and UV radiation were monitored every second with a broadband solar radiometer (ELDONET, Real Time Computer, Germany) and the averaged values over one-minute intervals were recorded.

2.4. Determination of photosynthetic rates

Samples in 50 mL quartz tubes were inoculated with 50 µL - 2.5 µCi (0.0925 MBq) of $NaH^{14}CO_3$ (ICN Radiochemicals, Irvine, California, USA) under a dim light condition. At the end of the incubations, samples were immediately filtered onto Whatman GF/F glass fiber filters (25 mm) under dim light, put into 20 mL scintillation vials, exposed to HCl fumes overnight and dried (45 °C) to remove the non-incorporated inorganic carbon. Then, 3 mL of scintillation cocktail (Hisafe 3, Perkin-Elmer) was added to each vial and the assimilated radiocarbon was counted using a liquid scintillation counter (Tri-Carb 2800TR, Perkin-Elmer) (Holm-Hansen and Helbling, 1995).

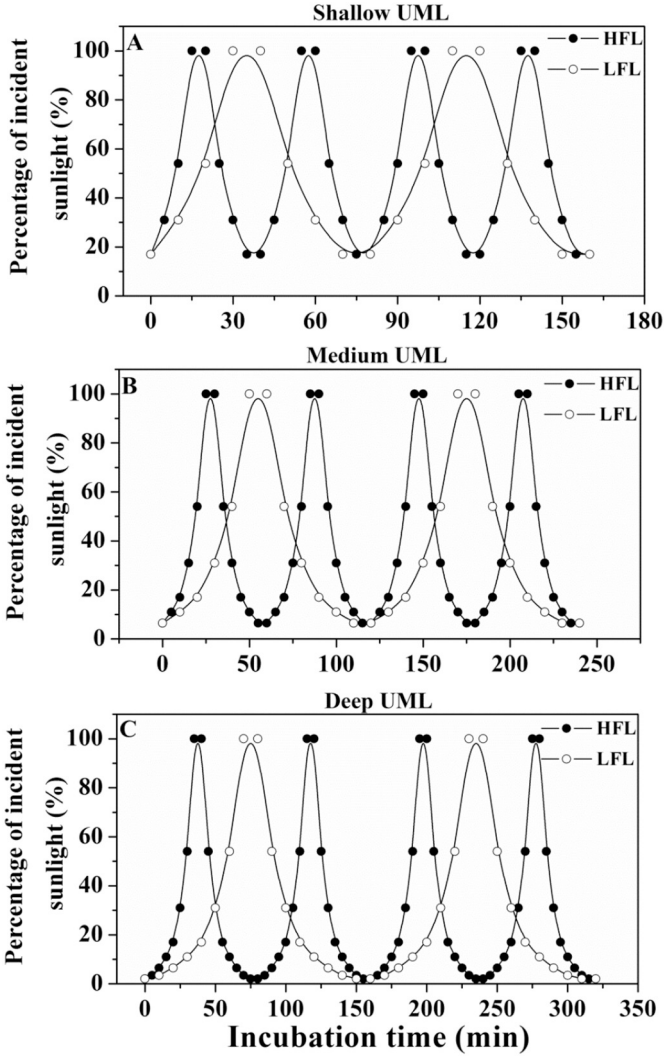

Fig. 2. Applied irradiances (percentage of incident solar radiation) during outdoor experiment periods under stimulated shallow (A), medium (B) and deep (C) upper mixed layer depth conditions. Solid and open symbols represent highly fluctuating light (HFL) and lowly fluctuating light (LFL), respectively.

Table 1
Average photosynthetically active radiation (PAR), ultraviolet A (UV-A) and ultraviolet B (UV-B) levels ($W\,m^{-2}$) during the outdoor incubations under various treatments.

Treatment	PAR ($W\,m^{-2}$)	UV-A ($W\,m^{-2}$)	UV-B ($W\,m^{-2}$)
Shallow UML-HFL	316.5	47.0	1.5
Shallow UML-LFL	249.1	42.4	1.5
Medium UML-HFL	201.6	33.9	1.1
Medium UML-LFL	151.9	26.2	1.0
Deep UML-HFL	270.1	41.0	1.3
Deep UML-LFL	150.7	26.0	0.9

2.5. Determination of cell numbers and chlorophyll a content

Cell numbers were counted every 24 h before and after renewal of medium, using a particle counter (Z2, Beckman instruments, Florida, US). Chlorophyll *a* content was determined by filtering the cultures

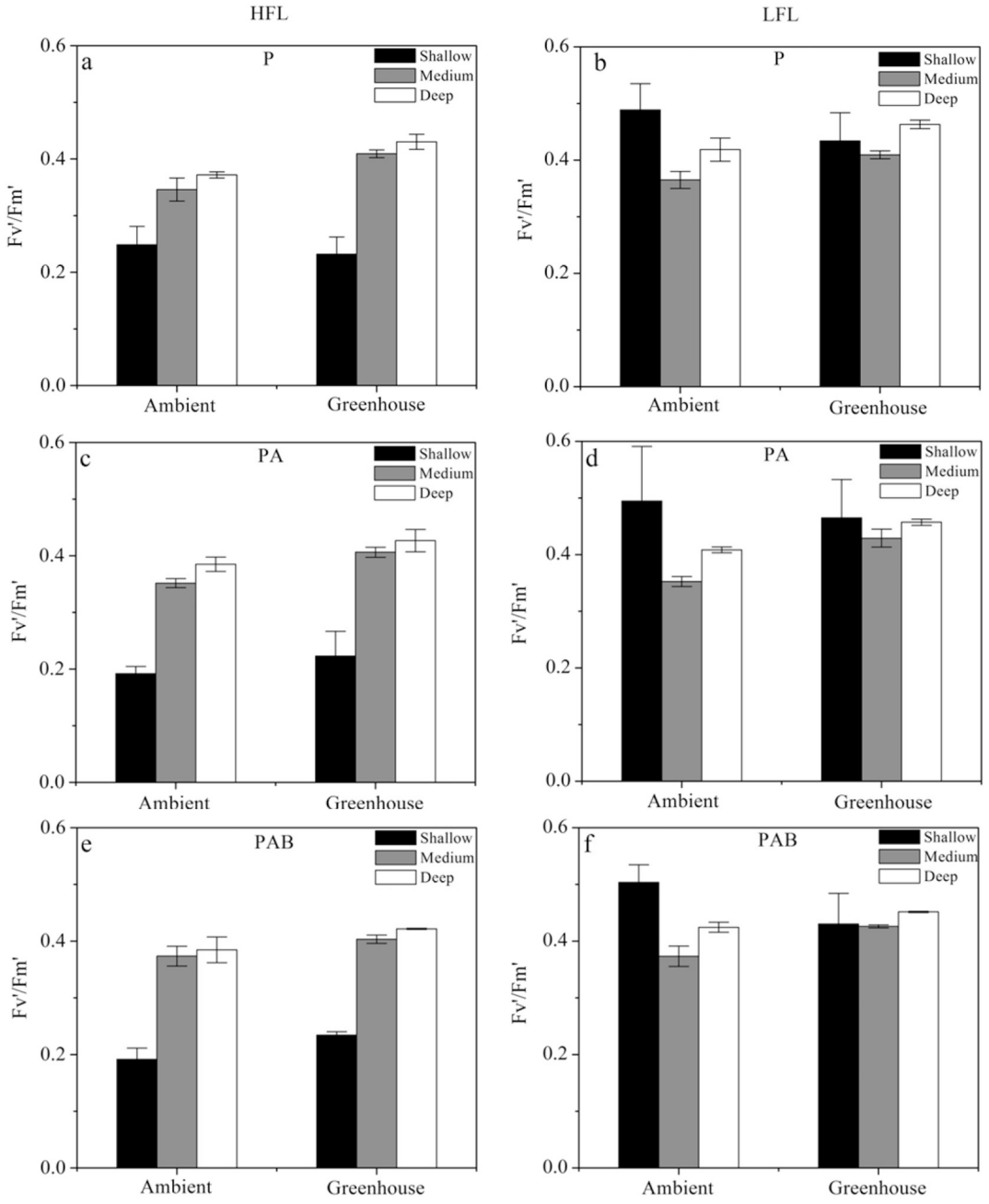

Fig. 3. The effective photochemical quantum yield (F_v'/F_m') of *Gephyrocapsa oceanica* cells in ambient and greenhouse conditions in highly fluctuating light (HFL) (a, c, e) and lowly fluctuating light (LFL) (b, d, f). Panels a and b, c and d, and e and f are the cells exposed to P (PAR), PA (PAR + UV-A) and PAB (PAR + UV-A + UV-B), respectively. Dark, grey and white columns indicate the cells under stimulated shallow, medium and deep upper mixed layer (UML) depth, respectively. Vertical bars are means ± standard deviations of triplicate incubations.

onto Whatman GF/F filters (25 mm), extracting overnight in absolute methanol, centrifuging (10 min at 6000 × *g*), measuring the absorbance of the supernatant over a scan between 200 and 800 nm with a spectrophotometer and calculating the concentration of the photosynthetic pigment following the equation of Porra (2002).

2.6. Evaluation of photochemical performance

The chlorophyll *a* fluorescence parameters, effective photochemical quantum yield (F_v'/F_m') and effective absorption cross-section of PSII (σ_{PSII}', A^2 quanta^{-1}), measured from samples taken at the end of the incubations, were determined in the light-exposed cells using a Fluorescence Induction and Relaxation device (FIRe) (Satlantic, Halifax, NS Canada) with application of a single saturating turn-over flash (80 µs, 5×10^4 µmol photons $m^{-2}\,s^{-1}$). The actinic light density was set according to the incident sunlight levels that the cells were exposed to during the experimental periods. Non-photochemical quenching (NPQ) was calculated as $NPQ = (F_m - F_m')/F_m'$, where F_m represents the maximum fluorescence yield after the samples were dark-adapted for 10 min, and F_m' represents the instant maximal fluorescence under the light.

2.7. Data analysis

Values of F_v'/F_m', Fm, F0, F_m' and σ_{PSII}' were determined from the fluorescence saturation curves analysed with MATLAB software using

Table 2
Three or four-way ANOVA analysis of individual and interactive effects among a combination of CO_2 and temperature (greenhouse, G), UML depth (D), solar radiation (R) and fluctuating frequency (F) on effective photochemical efficiency (F_v'/F_m'), non-photochemical quenching (NPQ), functional absorption cross section of photosystem II (PSII) (σ_{PSII}', A^2 quanta^{-1}) and photosynthetic carbon fixation rate (pg C cell^{-1} h^{-1}) in *Gephyrocapsa oceanica*.

Response	Treatment	df	*F*	*p*
F_v'/F_m'	R	2	0.110	0.896
	G	1	23.418	< **0.001**
	D	2	60.594	< **0.001**
	F	1	308.285	< **0.001**
	G × R	2	0.872	0.422
	R × D	4	0.349	0.844
	G × D	2	15.826	< **0.001**
	R × F	2	0.371	0.691
	G × F	1	3.621	0.061
	D × F	2	180.404	< **0.001**
	G × R × D	4	0.612	0.655
	G × R × F	2	0.381	0.685
	R × D × F	4	1.095	0.365
	G × F × D	2	5.208	**0.008**
	G × R × D × F	4	0.700	0.595
NPQ	R	2	2.543	0.086
	G	1	49.046	< **0.001**
	D	2	272.732	< **0.001**
	F	1	1.472	0.229
	G × R	2	0.619	0.541
	R × D	4	2.084	0.092
	G × D	2	0.428	0.653
	R × F	2	2.904	0.061
	G × F	1	15.509	< **0.001**
	D × F	2	0.333	0.718
	G × R × D	4	0.954	0.438
	G × R × F	2	0.115	0.891
	R × D × F	4	1.095	0.365
	G × F × D	2	4.475	**0.015**
	G × R × D × F	4	0.647	0.631
σ_{PSII}'	R	2	3.446	**0.037**
	G	1	1.059	0.307
	D	2	360.513	< **0.001**
	F	1	5.845	**0.018**
	G × R	2	4.906	**0.010**
	R × D	4	3.180	**0.018**
	G × D	2	4.784	**0.011**
	R × F	2	2.689	0.075
	G × F	1	10.478	**0.002**
	D × F	2	24.150	< **0.001**
	G × R × D	4	4.557	**0.002**
	G × R × F	2	2.224	0.116
	R × D × F	4	5.002	**0.001**
	G × F × D	2	12.212	< **0.001**
	G × R × D × F	4	4.941	**0.001**
Photosynthesis	R	2	4.864	**0.010**
	G	1	519.951	< **0.001**
	D	2	9.265	< **0.001**
	F	1	361.734	< **0.001**
	G × R	2	2.530	0.087
	R × D	4	1.150	0.340
	G × D	2	11.805	< **0.001**
	R × F	2	0.610	0.546
	G × F	1	30.714	< **0.001**
	D × F	2	44.442	< **0.001**
	G × R × D	4	1.201	0.318
	G × R × F	2	0.498	0.610
	R × D × F	4	0.942	0.445
	G × F × D	2	14.481	< **0.001**
	G × R × D × F	4	0.295	0.880

The p values in bold indicate the interactions between or among the factors are significant.

the Fireworx program, with instrument-specific light calibration factors. Individual or interactive effects between CO_2 & temperature, stimulated UML depth, light fluctuating frequency and UVR were analysed using one-, two-, three- and four-way ANOVA to establish significant difference ($p < 0.05$). Tukey HSD test was used for post-hoc comparisons. Pair-wise tests were conducted with one-way ANOVA.

3. Results

3.1. Solar irradiance

During the duration of the experiments, the average light density of PAR during the incubation periods ranged from 150.7 to 316.5 W m^{-2} (Table 1, Supplementary Fig. S1). Daily average UV-A and UV-B ranged from 26.0 to 47.0 Wm^{-2}, and 0.9 to 1.5 W m^{-2}, respectively (Table 1, Supplementary Fig. S1). Cells under deep UML depth with HFL received the highest PAR, UV-A and UV-B level, which was 316.5, 47.0 and 1.5 W m^{-2}, respectively (Table 1). Cells under deep UML depth with LFL received the lowest PAR, UV-A and UV-B level, which was 150.7, 26.0 and 0.9 W m^{-2}, respectively (Table 1).

3.2. Photochemical performance

The F_v'/F_m' of *G. oceanica* was significantly inhibited by ~50% within decreased UML depth both at ambient and greenhouse treatments regardless of the presence of UVR at HFL of 5 min (Four-way ANOVA, $F_{2,107} = 60.594$, $p < 0.001$) (Fig. 3a, c and e, Table 2). However, these negative effects were mitigated by the decreased light fluctuating frequency at LFL of 10 min (Four-way ANOVA, $F_{2,107} = 60.594$, $p < 0.001$) (Fig. 3b, d, and f, Table 2). Thus, there was a significant interaction between UML depth and light fluctuating frequency ($F_{2,107} = 180.404$, $p < 0.001$). Both increase in CO_2 level and temperature (i.e. greenhouse treatment) increased F_v'/F_m' ($F_{1,107} = 23.418$, $p < 0.001$), however, UVR did not result in any significant effect on it ($F_{2,107} = 0.110$, $p = 0.896$) (Table 2).

Decreasing UML depth significantly increased the σ_{PSII}' of *G. oceanica* (Four-way ANOVA, $F_{2,107} = 360.513$, $p < 0.001$), with an average of ~400 A^2 quanta^{-1} in deep UML depth treatment and ~1000 A^2 quanta^{-1} in shallow UML depth treatment (Fig. 4, Table 2). Being different from that of F_v'/F_m', σ_{PSII}' was not affected by both increasing in CO_2 level and temperature (i.e. greenhouse treatment) ($F_{1,107} = 1.059$, $p = 0.307$), but was increased in the presence of UVR ($F_{2,107} = 3.446$, $p = 0.037$) (Fig. 4, Table 2), within higher enhancement in shallow UML depth treatment, indicating a significant interaction between UVR and UML depth ($F_{4,107} = 3.180$, $p = 0.018$). In addition, the 3-way interaction (UVR × CO_2&temperature × UML depth) test was significant ($F_{4,107} = 4.557$, $p = 0.002$), indicating that the interaction between UVR and UML depth was greater at greenhouse treatment than at ambient one.

Both increase in CO_2 level and temperature ($F_{1,107} = 49.046$, $p < 0.001$) and decrease of UML depth ($F_{2,107} = 272.732$, $p < 0.001$) significantly increased NPQ regardless of the presence of UVR or light fluctuating frequency (Fig. 5, Table 2). Decrease of UML depth increased NPQ by ~5–8 times compared to that in the stimulated deeper one (Fig. 5). The significant interaction between increased CO_2&temperature and decreased light fluctuating frequency suggested that these two drivers synergistically increased the NPQ of *G. oceanica* ($F_{2,107} = 15.509$, $p < 0.001$). In addition, the 3-way interaction (light fluctuating frequency × CO_2&temperature × UML depth) test was significant ($F_{2,107} = 4.475$, $p = 0.015$), indicating that the interaction between CO_2&temperature and light fluctuating frequency was greater at shallow UML depth than under deep UML depth condition (Fig. 5, Table 2).

3.3. Photosynthetic carbon fixation rate

In general, four variables of CO_2&temperature, light fluctuating frequency, UML depth and UVR all have a significant effect on the photosynthetic carbon fixation rate of *G. oceanica* (all $p < 0.05$, Table 2) (Fig. 6). Specifically, both increasing levels of CO_2 level and

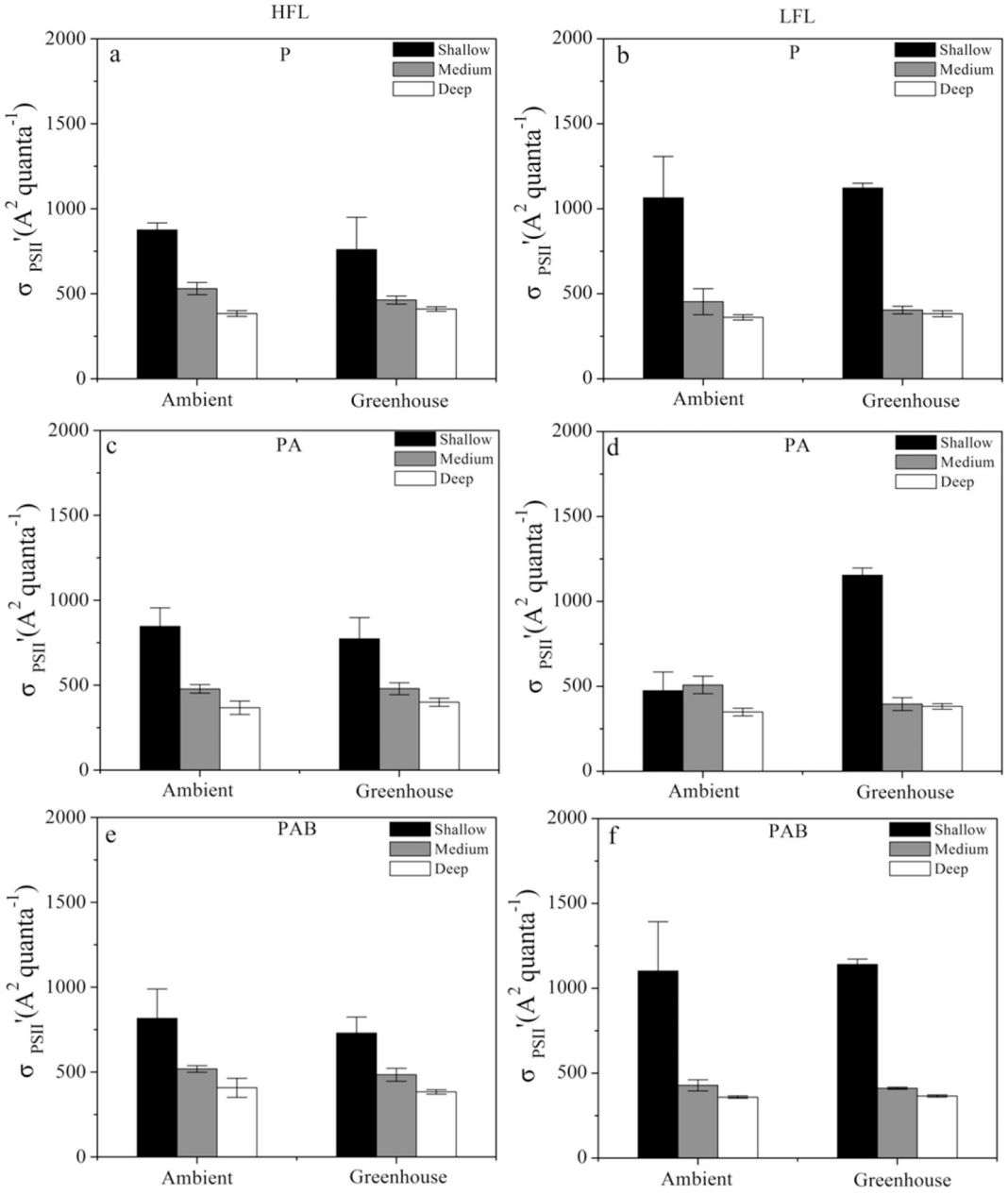

Fig. 4. The effective absorption cross-section of PSII (σ_{PSII}', A^2 quanta^{-1}) of *Gephyrocapsa oceanica* cells in ambient and greenhouse conditions in highly fluctuating light (HFL) (a, c, e) and lowly fluctuating light (LFL) (b, d, f). Panels a and b, c and d, and e and f are the cells exposed to P (PAR), PA (PAR + UV-A) and PAB (PAR + UV-A + UV-B), respectively. Dark, grey and white columns indicate the cells under stimulated shallow, medium and deep upper mixed layer (UML) depth, respectively. Vertical bars are means ± standard deviations of triplicate incubations.

temperature significantly increased the photosynthetic carbon fixation rates of *G. oceanica* by ~58% to ~82% ($F_{1,107} = 519.951$, $p < 0.001$) (Fig. 6). Highly light fluctuating frequency of 5 min significantly decreased the photosynthetic carbon fixation rates by ~34% to 37%, with an average value of 0.05 pg C cell^{-1} h^{-1} ($F_{1,107} = 361.734$, $p < 0.001$). A significant interaction between rising CO_2&temperature and increasing light fluctuating frequency suggested that these two drivers act synergistically to increase the photosynthetic carbon fixation rates of *G. oceanica* ($F_{1,107} = 30.714$, $p < 0.001$). However, increasing light fluctuating frequency and shoaling of UML depth acted antagonistically to increase the photosynthetic carbon fixation rates ($F_{2,107} = 44.442$, $p < 0.001$).

3.4. Comparisons of responses to contemporary and future scenario-based conditions

We used the conditions of 400 μatm CO_2, 20 °C and deep upper mixed layer (2% of sea surface incident light level) to present the "current" day conditions, and the conditions of 1000 μatm CO_2, 25 °C and deep upper mixed layer (17% of sea surface incident light level) to show the future conditions as projected by the high-emission scenario (RCP 8.5, IPCC, 2014) for 2100 (Table 3). Based on the percentage changes in physiological responses, our results showed that the photochemical efficiency of F_v'/F_m' significantly decreased by ~40% in future conditions during daytime. At the same time, the cells may

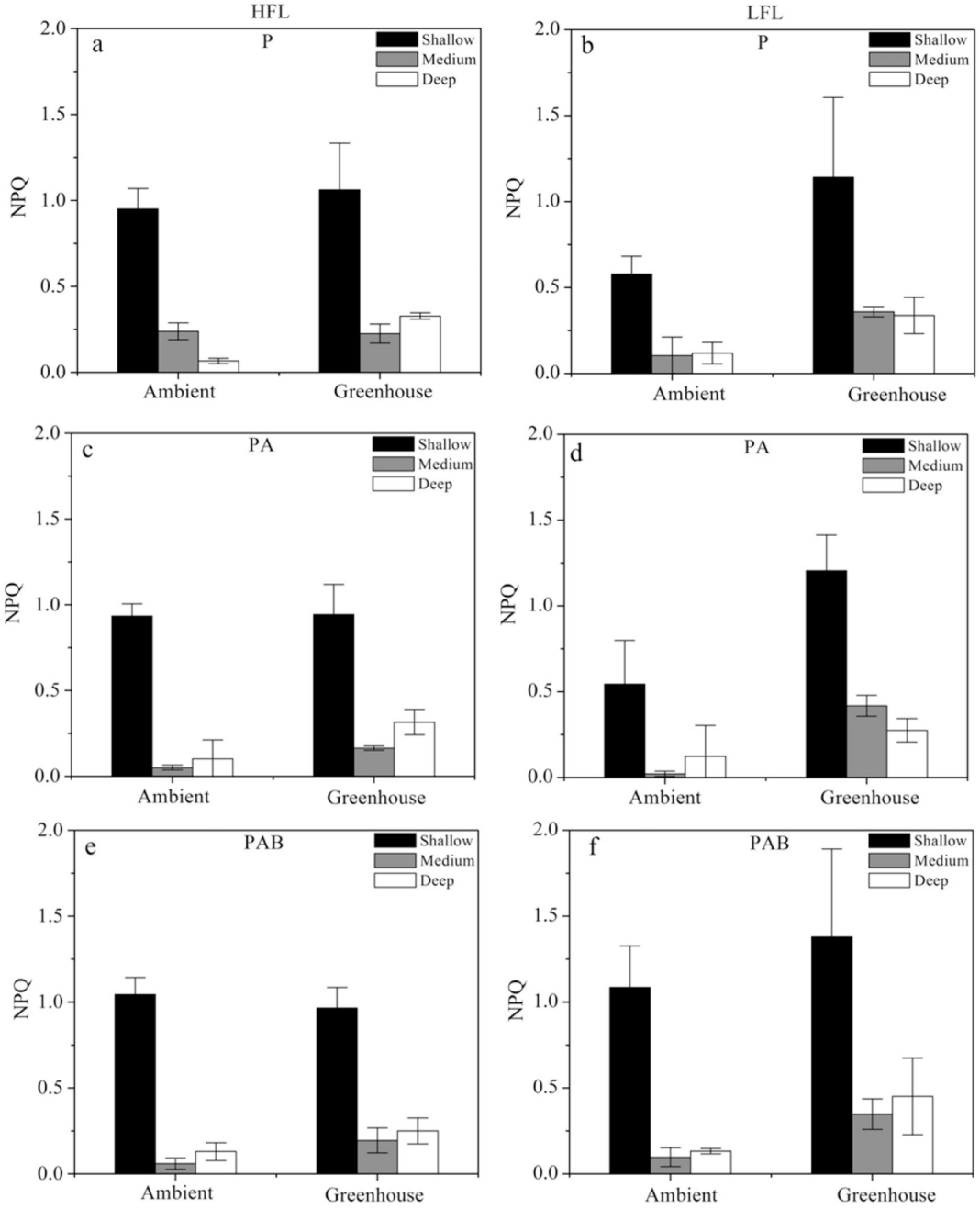

Fig. 5. Non-photochemical quenching (NPQ) of *Gephyrocapsa oceanica* cells in ambient and greenhouse conditions in highly fluctuating light (HFL) (a, c, e) and lowly fluctuating light (LFL) (b, d, f). Panels a and b, c and d, and e and f are the cells exposed to P (PAR), PA (PAR + UV-A) and PAB (PAR + UV-A + UV-B), respectively. Dark, grey and white columns indicate the cells under stimulated shallow, medium and deep upper mixed layer (UML) depth, respectively. Vertical bars are means ± standard deviations of triplicate incubations.

exhibit higher light stress (higher NPQ) with higher daytime-integrated light exposure in future upper mixed layer (Table 3). Nevertheless, the cells under future conditions may increase their functional antennae sizes (~80%–230%) and lead to enhanced photosynthesis (~34%–163%) (Table 3).

4. Discussion

In parallel with the shoaling of UML depth, the cells of *G. oceanica* could be photoinhibited, leading to a decrease in F_v'/F_m' and increasing in NPQ, since the exposed PAR level reached up to 283 W m^{-2} (~1300 μmol photons m^{-2} s^{-1}), which exceeds growth-saturating light level (200 μmol photons m^{-2} s^{-1}) of this species (Zhang et al., 2015). The excessive light should be responsible for the increased effective absorption cross sections (Fig. 4), reflecting antenna connectivity. When PSII reaction centers close or become photoinactivated, the antenna complex may serve adjacent antennae connected to open functional PSII centers, causing a dynamically increasing effective antenna size (Hecks et al., 1996; Stirbet et al., 1998; Six et al., 2009). It is considered as one of the mechanisms against PSII photoinhibition for photosynthetic organisms to cope with light fluctuations (Six et al., 2009).

Many factors are known to modulate effects of light on physiological performance of coccolithophores, such as CO_2 level (Zondervan et al., 2002; Rokitta and Rost, 2012; Zhang et al., 2015; Jin et al., 2017), temperature (Feng et al., 2008), nitrogen source (Tong et al., 2016) and

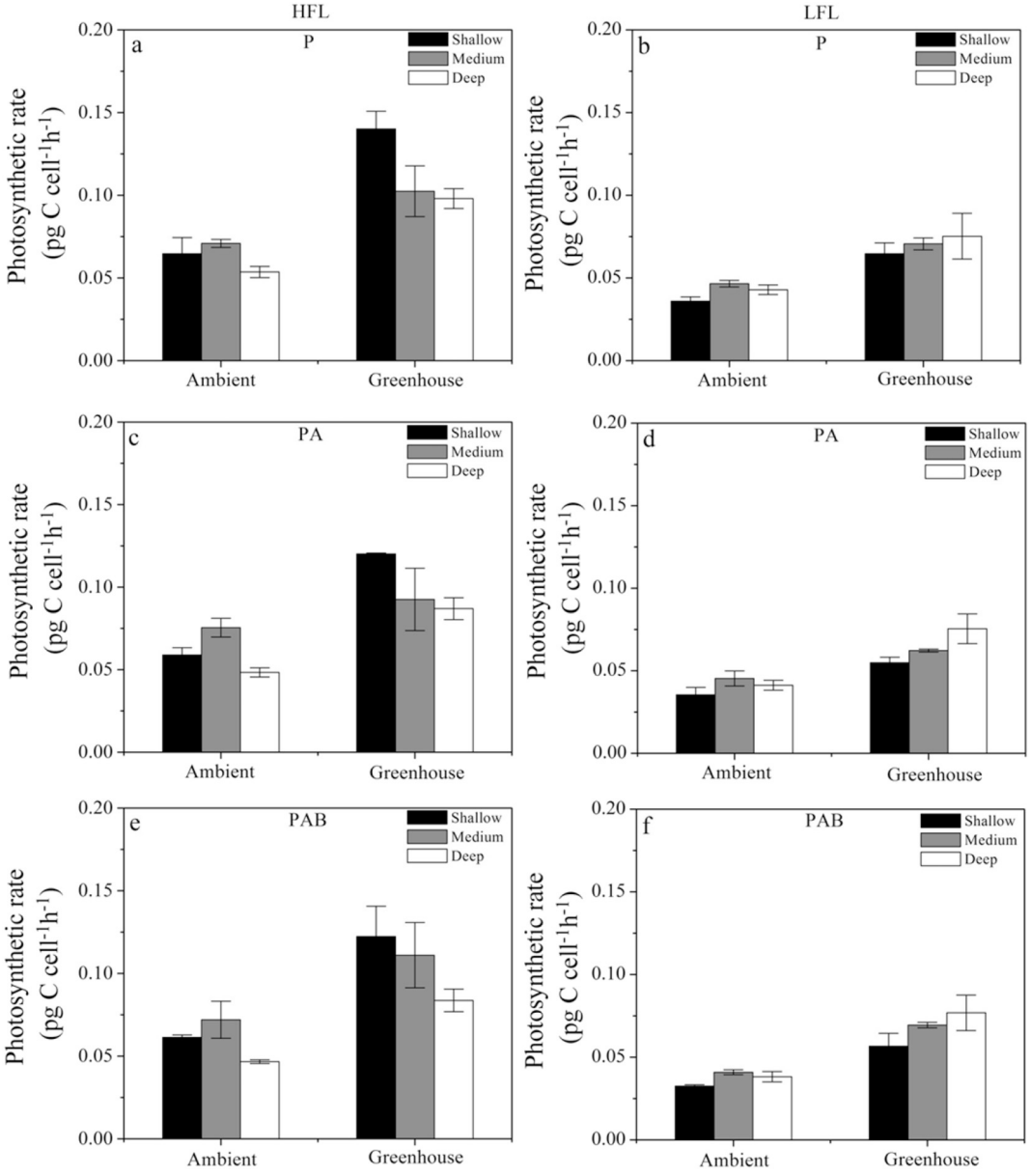

Fig. 6. Photosynthetic carbon fixation rates (pg C cell^{-1} h^{-1}) of *Gephyrocapsa oceanica* cells in ambient and greenhouse conditions in highly fluctuating light (HFL) (a, c, e) and lowly fluctuating light (LFL) (b, d, f). Panels a and b, c and d, and e and f are the cells exposed to P (PAR), PA (PAR + UV-A) and PAB (PAR + UV-A + UV-B), respectively. Dark, grey and white columns indicate the cells under stimulated shallow, medium and deep upper mixed layer (UML) depth, respectively. Vertical bars are means ± standard deviations of triplicate incubations.

calcium concentrations (Trimborn et al., 2007). In the present work, for the first time, we demonstrated that the negative effects of high light on the photosynthetic activity of coccolithophores could be offset by decreased frequency of fluctuating light (Figs. 3–6). Since energetic costs for maintenance and repair associated with highly fluctuating light can be higher than under less fluctuating conditions (Dimier et al., 2009), so we observed higher F_v'/F_m' values at lowly fluctuating light conditions as more energy would be used for photo-damage repair processes in this case (Fig. 2). Fluctuating light may interactively act with rising CO_2 level to affect coccolithophores' physiology due to interplays between light-dependent and independent reactions of photosynthesis. For instance, a combination of rising CO_2 level and fluctuating light decreased the carbon fixation when compared with that of ambient CO_2 level and constant light in the same species used in the present study (Jin et al., 2013). Consequently, these three environmental drivers of light intensity, CO_2 level and fluctuating irradiances may have the potential to interactively influence coccolithophores' physiology (e.g. photosynthetic activity in the present study), though mechanisms involved in these interactions need to be explored.

The photosynthetic carbon fixation rates and photosynthetic activity in the "greenhouse" treatments were significantly higher than that in the "ambient" treatments (Fig. 6). This finding is in good agreement with previous studies that examined the combined effect of increased CO_2 level and temperature on particulate organic carbon (POC) content and primary production of coccolithophores (Feng et al., 2008; De Bodt et al., 2010; Borchard et al., 2011; Benner et al., 2013). Since *G. oceanica* showed increases in POC content and growth at elevated CO_2 concentration of 1000 μatm at 20 °C (Jin et al., 2013), further increase in temperature to 25 °C did not reverse this trend, suggesting that the increased temperature resulted in additive effect with the elevated CO_2. Although the thermal responses of coccolithophores depend on strain- or species-specific temperature optimum (Fisher and Honjo, 1989, Matson et al., 2016) and isolation locations (Zhang et al., 2014), we concluded that the experimental temperature of 25 °C is

Table 3
Comparisons of effective photochemical efficiencies (F_v'/F_m') and photosynthetic carbon fixation rates (pg C cell^{-1} h^{-1}) of *Gephyrocapsa oceanica* between "current" and "future" day conditions. "Current" presents the present conditions, that was 400 μatm CO_2, 20 °C and deep upper mixed layer (2% of sea surface incident light level); "Future" presents the future conditions that projected by high-emission scenario (RCP 8.5, IPCC, 2014) for 2100, that was 1000 μatm CO_2, 25 °C and shallow upper mixed layer (17% of sea surface incident light level). Effect of "+" represents an increase and "−" represents a decrease in the future, respectively. Statistical analyses between "current" and "future" were performed by one-way ANOVA. "ns" indicates that there was no significant difference between that of "current" and "future" days conditions.

Physiological responses		High turnover rate of fluctuating light (HFL)			Low turnover rate of fluctuating light (LFL)		
		PAB	PA	P	PAB	PA	P
F_v'/F_m'	Current	0.385 ± 0.023	0.385 ± 0.013	0.372 ± 0.006	0.424 ± 0.009	0.408 ± 0.005	0.419 ± 0.021
	Future	0.234 ± 0.006	0.223 ± 0.044	0.232 ± 0.030	0.430 ± 0.054	0.465 ± 0.068	0.434 ± 0.050
	Change (%)	39%	42%	38%	1%	14%	4%
	Effects (+/−)	−	−	−	ns	ns	ns
	Stats	$F = 123.7$, $p < 0.001$	$F = 37.92$, $p = 0.004$	$F = 61.79$, $p = 0.001$	$F = 0.033$, $p = 0.865$	$F = 2.079$, $p = 0.223$	$F = 0.246$, $p = 0.646$
Photosynthesis	Current	0.047 ± 0.001	0.048 ± 0.003	0.054 ± 0.003	0.038 ± 0.003	0.041 ± 0.003	0.043 ± 0.003
	Future	0.122 ± 0.018	0.120 ± 0.000	0.141 ± 0.011	0.122 ± 0.057	0.055 ± 0.003	0.065 ± 0.007
	Change (%)	163%	149%	163%	50%	34%	51%
	Effects (+/−)	+	+	+	+	+	+
	Stats	$F = 51.0$, $p = 0.002$	$F = 1980$, $p < 0.001$	$F = 182$, $p < 0.001$	$F = 14.6$, $p = 0.019$	$F = 27.48$, $p = 0.006$	$F = 28.22$, $p = 0.006$
NPQ	Current	0.130 ± 0.052	0.103 ± 0.110	0.067 ± 0.015	0.132 ± 0.016	0.123 ± 0.181	0.119 ± 0.063
	Future	0.966 ± 0.120	0.943 ± 0.176	1.063 ± 0.271	1.380 ± 0.511	1.205 ± 0.208	1.142 ± 0.464
	Change (%)	643%	816%	1423%	945%	880%	806%
	Effects (+/−)	+	+	+	+	+	+
	Stats	$F = 122.6$, $p < 0.001$	$F = 49.24$, $p = 0.001$	$F = 40.48$, $p = 0.003$	$F = 17.91$, $p = 0.013$	$F = 46.25$ $p = 0.002$	$F = 14.30$, $p = 0.019$
σ_{PSII}'	Current	408 ± 56	368 ± 39	384 ± 17	359 ± 7	348 ± 23	361 ± 16
	Future	730 ± 95	774 ± 124	760 ± 189	1141 ± 31	1155 ± 42	1122 ± 29
	Change (%)	79%	110%	98%	218%	232%	211%
	Effects (+/−)	+	+	+	+	+	+
	Stats	$F = 25.57$, $p = 0.007$	$F = 29.24$, $p = 0.006$	$F = 11.76$, $p = 0.027$	$F = 1785$, $p < 0.001$	$F = 840.9$, $p < 0.001$	$F = 1647$, $p < 0.001$

shifted towards but not away from the temperature optimum of this species. Mechanistically, transcripts encoded with a mitochondrial oxoglutarate/malate carrier protein and a flavin-containing monooxygenase were down-regulated, while those involved in cellular processes and signaling, information storage and processing and metabolism were not modulated when the coccolithophores were grown under elevated CO_2 and temperatures (Benner et al., 2013). For the increased photosynthetic activity in *G. oceanica* grown under elevated temperature and CO_2 conditions, on one hand, the energy saved from down-regulated operation of CCM as a result of elevated CO_2 (Jin et al., 2013) could be used for repair of photodamages. On the other hand, the stimulated photosynthetic performance appeared to be attributed to the extra carbon loss, i.e. extra electron drainage due to enhanced respiration (Jin et al., 2015), which provides a protective role (Li et al., 2012). These two drivers (CO_2 and temperature) may also have the potential to act interactively with other drivers (e.g. light intensity, UVR, fluctuating irradiance in present study) to influence the cellular processes of coccolithophores, and the mechanisms involved in these interactions, remain to be studied.

UVR is known to affect the photosynthetic carbon fixation, calcification, photophysiological performance and growth of coccolithophores (Gao et al., 2009; Jin et al., 2013; Xu and Gao, 2015). In the present work, presence of UVR decreased the photosynthetic carbon fixation rates of *G. oceanica* (Fig. 5), being consistent with previous studies (e.g. Xu and Gao, 2015). Xu and Gao (2015) also demonstrated that the effects of UVR on the photosynthetic carbon fixation depended on the mean PAR levels, with no significant effects of UVR on POC production rates at the PAR level of 248 μmol photons m^{-2} s^{-1}, while UVR decreased the POC production rates at the PAR level of 398 μmol photons m^{-2} s^{-1}, which is comparable with that of present study. Our data showed that presence of UVR increased the effective absorption cross sections, with more pronounced effects at high PAR/UVR level, suggesting that PSII reaction centers close or become photoinactivated not only due to the high PAR intensity, but also due to high level of UVR. Therefore, the antenna complex serves adjacent antennae connected to open functional PSII centers, causing a dynamically increased effective antenna size (Fig. 4). Different from that of photosynthetic carbon fixation rates and σ_{PSII}', no significant effects of UVR on F_v'/F_m' or NPQ were found in our study. It was probably due to the fact that photosynthetic organisms have evolved a range of strategies to mitigate UVR damage including increasing UVR-screening pigments (e.g., Klisch et al., 2002), UVB-absorbing/blocking secondary metabolites (e.g. phlorotannin compounds) and DNA repair systems as photolyase activity against UVR-induced DNA damage (e.g. Van De Poll et al., 2001; Roleda et al., 2004).

The ongoing ocean warming and acidification with decreasing thickness of UML that exposes phytoplankton cells to higher exposures of UVR as well as PAR are the key ocean climate drivers, that could bring about profound impacts on marine ecosystems (Boyd et al., 2019). For coccolithophores like *G. oceanica*, elevated levels of CO_2 and temperature might increase their photosynthetic carbon fixation, which, however, might be damped or enhanced by other environmental drivers such as light intensity, fluctuating light frequency and UVR as shown in the present study and a recent study on *Emiliania huxleyi* (Tong et al., 2019). Nutrient availabilities are also likely to alter the responses of coccolithophores and other phytoplankton species to ocean acidification and warming (Li et al., 2018). The species used in the present study is non-calcifying, therefore, our results could not reflect the impacts of multiple drivers on calcification of coccolithophores. However, there are no doubts that calcification of coccolithophores will be impacted by the multiple drivers employed in the present work, since they did influence photosynthetic performances that calcification depends on. In addition, biochemical composition of coccolithophore (e.g. fatty acid composition, phenolic compounds) has been shown to be significantly altered under elevated CO_2 condition, and these changes could transfer up to secondary producers via trophic energy and nutrient transfer (Rossoll et al., 2012; Schoo et al., 2013; Jin et al., 2015). Therefore, further knowledge is needed to understand the consequences

of multiple environmental drivers on food webs and marine biological CO_2 pumps.

Supplementary data to this article can be found online at https://doi.org/10.1016/j.marpolbul.2019.06.032.

Acknowledgments

This study was supported by National Natural Science Foundation of China (41806141, 41720104005, 41721005, 41430967) and joint project of National Natural Science Foundation of China and Shandong Province (No. U1606404).

References

Benner, I., Diner, R.E., Lefebvre, S.C., Li, D., Komada, T., Carpenter, E.J., Stillman, J.H., 2013. *Emiliania huxleyi* increases calcification but not expression of calcification-related genes in long-term exposure to elevated temperature and pCO_2. Philos. Trans. R. Soc. B 368, 20130049. https://doi.org/10.1098/rstb.2013.0049.

Borchard, C., Borges, A.V., Händel, N., Engel, A., 2011. Biogeochemical response of *Emiliania huxleyi* (PML B92/11) to elevated CO_2 and temperature under phosphorous limitation: a chemostat study. J. Exp. Mar. Biol. Ecol. 410, 61–71.

Boyd, P.W., Brown, C.J., 2015. Modes of interactions between environmental drivers and marine biota. Front. Mar. Sci. 2.

Boyd, P.W., Hutchins, D.A., 2012. Understanding the responses of ocean biota to a complex matrix of cumulative anthropogenic change. Mar. Ecol. Prog. Ser. 470, 125–135.

Boyd, P.W., Collins, S., Dupont, S., Fabricius, K., Gattuso, J.P., Havenhand, J., Hutchins, D.A., Riebesell, U., Rintoul, M.S., Vichi, M., 2018. Experimental strategies to assess the biological ramifications of multiple drivers of global ocean change-a review. Glob. Chang. Biol. 1–23.

Boyd, P.W., Strzepek, R., Fu, F.X., Hutchins, D.A., 2010. Environmental control of open-ocean phytoplankton groups: Now and in the future. Limnol. Oceanogr 55, 1353–1376.

Boyd, P.W., Collins, S., Dupont, S., Fabricius, K., Gattuso, J.-P., Havenhand, J., Hutchins, D.A., McGraw, C.M., Riebesell, U., Vichi, M., Biswas, H., Ciotti, A., Dillingham, P., Gao, K., Gehlen, M., Hurd, C.L., Kurihawa, H., Navarro, J., Nilsson, G.E., Passow, U., Pörtner, H.-O., 2019. SCOWG149 Handbook to Support the SCOR Best Practice Guide for 'Multiple Drivers' Marine Research. https://doi.org/10.25959/5c92fdf0d3c7a.

Brennan, G., Collins, S., 2015. Growth responses of a green alga to multiple environmental drivers. Nat. Clim. Chang. 5, 892–897.

De Bodt, C., Van Oostende, N., Harlay, J., Sabbe, K., Chou, L., 2010. Individual and interacting effects of pCO_2 and temperature on *Emiliania huxleyi* calcification: study of the calcite production, the coccolith morphology and the coccosphere size. Biogeosciences 7, 1401–1412.

Dimier, C., Brunet, C., Geider, R., Raven, J., 2009. Growth and photoregulation dynamics of the picoeukaryote *Pelagomonas calceolata* in fluctuating light. Limnol. Oceanogr. 54, 823–836.

Feng, Y., Warner, M.E., Zhang, Y., Sun, J., Fu, F.-X., Rose, J.M., Hutchins, D.A., 2008. Interactive effects of increased pCO_2, temperature and irradiance on the marine coccolithophore *Emiliania huxleyi* (Prymnesiophyceae). Eur. J. Phycol. 43, 87–98.

Feng, Y., Roleda, M.Y., Armstrong, E., Boyd, P.W., Hurd, C.L., 2017. Environmental controls on the growth, photosynthetic and calcification rates of a Southern Hemisphere strain of coccolithophore *Emiliania huxleyi*. Limnol. Oceanogr. 62, 519–540.

Fisher, N.S., Honjo, S., 1989. Intraspecific differences in temperature and salinity responses in the coccolithophore *Emiliania huxleyi*. Biol. Oceanogr. 6, 355–361.

Gao, K., Ruan, Z., Villafañe, V.E., Gattuso, J.P., Helbling, E.W., 2009. Ocean acidification exacerbates the effect of UV radiation on the calcifying phytoplankter *Emiliania huxleyi*. Limnol. Oceanogr. 54, 1855–1862.

Gao, K., Helbling, E.W., Häder, D.-P., Hutchins, D.A., 2012. Responses of marine primary producers to interactions between ocean acidification, solar radiation, and warming. Mar. Ecol. Prog. Ser. 470, 167–189. https://doi.org/10.3354/meps10043.

Gunderson, A.R., Armstrong, E.J., Stillman, J.H., 2016. Multiple stressors in a changing world: the need for an improved perspective on physiological responses to the dynamic marine environment. Annu. Rev. Mar. Sci. 8, 357–378.

Hecks, B., Wilhelm, C., Trissl, H.-W., 1996. Functional organization of the photosynthetic apparatus of the primitive alga *Mantoniella squamata*. Biochim. Biophys. Acta 1274, 21–30.

Helbling, E.W., Gao, K., Goncalves, R.J., Wu, H., Villafañe, V.E., 2003. Utilization of solar UV radiation by coastal phytoplankton assemblages off SE China when exposed to fast mixing. Mar. Ecol. Prog. Ser. 259, 59–66.

Holm-Hansen, O., Helbling, E.W., 1995. Técnicas para la medición de la productividad primaria en el fitoplancton. In: Alveal, K., Ferrario, M.E., Oliveira, E.C., Sar, E. (Eds.), Manual de Métodos Ficológicos. Universidad de Concepción, Concepción, Chile, pp. 329–350.

IPCC Climate Change, 2014. In: Field, C.B. (Ed.), Impacts, Adaptation, and Vulnerability. Part A: Global and Sectoral Aspects. Cambridge Univ. Press, pp. 2014.

Jin, P., Gao, K., 2016. Reduced resilience of a globally distributed coccolithophore to ocean acidification: confirmed up to 2000 generations. Mar. Pollut. Bull. 103, 101–108.

Jin, P., Gao, K., Villafañe, V.E., Campbell, D.A., Helbling, E.W., 2013. Ocean acidification alters the photosynthetic responses of a coccolithophorid to fluctuating ultraviolet and visible radiation. Plant Physiol. 162, 2084–2094.

Jin, P., Wang, T., Liu, N., Dupont, S., Beardall, J., Boyd, P.W., Riebesell, U., Gao, K., 2015. Ocean acidification increases the accumulation of toxic phenolic compounds across trophic levels. Nat. Commun. 6, 8714.

Jin, P., Ding, J., Xing, T., Riebesell, U., Gao, K., 2017. High levels of solar radiation offset impacts of ocean acidification on calcifying and non-calcifying strains of *Emiliania huxleyi*. Mar. Ecol. Prog. Ser. 568, 47–58.

Keeling, R.F., Körtzinger, A., Gruber, N., 2010. Ocean deoxygenation in a warming world. Annu. Rev. Mar. Sci. 2, 199–229.

Klisch, M., Sinha, R., Hfider, D.-P., 2002. UV-absorbing compounds in algae. Curr. Top. Plant Biol. 3, 113–120.

Langer, G., Geisen, M., Baumann, K.-H., Kläs, J., Riebesell, U., Thoms, S., Young, J.R., 2006. Species-specific responses of calcifying algae to changing seawater carbonate chemistry. Geochem. Geophys. Geosyst. 7, Q09006.

Langer, G., Nehrke, G., Probert, I., Ly, J., Ziveri, P., 2009. Strain-specific responses of *Emiliania huxleyi* to changing seawater carbonate chemistry. Biogeosciences 6, 4361–4383.

Li, Y., Gao, K., Villafañe, V., Helbling, E., 2012. Ocean acidification mediates photosynthetic response to UV radiation and temperature increase in the diatom *Phaeodactylum tricornutum*. Biogeosciences 9, 3931–3942.

Li, W., Yang, Y., Li, Z., Xu, J., Gao, K., 2017. Effects of seawater acidification on the growth rates of the diatom Thalassiosira (Conticribra) weissflogii under different nutrient, light, and UV radiation regimes. J. Appl. Phycol. 29, 133–142.

Li, F., Beardall, J., Gao, K., 2018. Diatom performance in a future ocean: interactions between nitrogen limitation, temperature, and CO_2-induced seawater acidification. ICES J. Mar. Sci. 75, 1451–1464.

Marra, J., 1978. Phytoplankton photosynthetic response to vertical movement in a mixed layer. Mar. Biol. 46, 203–208.

Matson, P.G., Ladd, T.M., Halewood, E.R., Sangodkar, R.P., Chmelka, B.F., Iglesias-Rodriguez, M.D., 2016. Intraspecific differences in biogeochemical responses to thermal change in the coccolithophore *Emiliania huxleyi*. PLoS ONE 9 (2), e88308.

Meyer, J., Riebesell, U., 2015. Reviews and syntheses: responses of coccolithophores to ocean acidification: a meta-analysis. Biogeosciences 12, 1671–1682.

Milner, S., Langer, G., Grelaud, M., Ziveri, P., 2016. Ocean warming modulates the effects of acidification on *Emiliania huxleyi* calcification and sinking. Limnol. Oceanogr. 61, 1322–1336.

Morel, F.M.M., Rueter, J., Anderson, D.M., Guillard, R., 1979. Aquil: a chemically defined phytoplankton culture medium for trace metal studies. J. Phycol. 15, 135–141.

Paasche, E., 1968. The effect of temperature, light intensity, and photoperiod on coccolith formation. Limnol. Oceanogr. 13, 178–181.

Paasche, E., 1999. Reduced coccolith calcite production under light-limited growth: a comparative study of three clones of *Emiliania huxleyi* (Prymnesiophyceae). Phycologia 38, 508–516.

Paasche, E., 2002. A review of the coccolithophorid *Emiliania huxleyi* (Prymnesiophyceae), with particular reference to growth, coccolith formation, and calcification-photosynthesis interactions. Phycologia 40, 503–529.

Porra, R.J., 2002. The chequered history of the development and use of simultaneous equations for the accurate determination of chlorophylls a and b. Photosynth. Res. 73, 149–156.

Raven, J.A., Crawfurd, K., 2012. Environmental controls on coccolithophore calcification. Mar. Ecol. Prog. Ser. 470, 137–166.

Riebesell, U., Gattuso, J.-P., 2015. Lessons learned from ocean acidification research. Nat. Clim. Chang. 5, 12–14.

Riebesell, U., Zondervan, I., Rost, B., Tortell, P.D., Richard, E.Z., Morel, F.M.M., 2000. Reduced calcification of marine plankton in response to increased atmospheric CO_2. Nature 407, 364–367.

Rokitta, S.D., Rost, B., 2012. Effects of CO_2 and their modulation by light in the life-cycle stages of the coccolithophore *Emiliania huxleyi*. Limnol. Oceanogr. 57, 607–618.

Roleda, M., van de Poll, W.H., Hanelt, D., Wiencke, C., 2004. PAR and UVBR effects on photosynthesis, viability, growth and DNA in different life stages of two coexisting Gigartinales: implications for recruitment and zonation pattern. Mar. Ecol. Prog. Ser. 281, 37–50.

Rossoll, D., Bermúdez, R., Hauss, H., Schulz, K.G., Riebesell, U., Sommer, U., Winder, M., 2012. Ocean acidification-induced food quality deterioration constrains trophic transfer. PLoS ONE 7, e34737.

Sarmiento, J., Slater, R., Barber, R., Bopp, L., Doney, S.C., Hirst, A., Kleypas, J., Matear, R., Mikolajewicz, U., Monfray, P., 2004. Response of ocean ecosystems to climate warming. Global Biogeochem Cy 18, GB3003.

Schmidtko, S., Stramma, L., Visbeck, M., 2017. Decline in global oceanic oxygen content during the past five decades. Nature 542, 335.

Schoo, K.L., Malzahn, A.M., Krause, E., Boersma, M., 2013. Increased carbon dioxide availability alters phytoplankton stoichiometry and affects carbon cycling and growth of a marine planktonic herbivore. Mar. Biol. 160, 2145–2155.

Sciandra, A., Harlay, J., Lefèvre, D., Lemé, R., Rimmelin, P., Denis, M., Gattuso, J.P., 2003. Response of coccolithophorid *Emiliania huxleyi* to elevated partial pressure of CO_2 under nitrogen limitation. Mar. Ecol. Prog. Ser. 261.

Sett, S., Bach, L.T., Schulz, K.G., Koch-Klavsen, S., Lebrato, M., Riebesell, U., 2014. Temperature modulates coccolithophorid sensitivity of growth, photosynthesis and calcification to increasing seawater pCO_2. PLoS ONE 9, e88308.

Shi, D., Xu, Y., Morel, F., 2009. Effects of the pH/pCO_2 control method on medium chemistry and phytoplankton growth. Biogeosciences 6, 1199–1207.

Six, C., Sherrard, R., Lionard, M., Roy, S., Campbell, D.A., 2009. Photosystem II and pigment dynamics among ecotypes of the green alga *Ostreococcus*. Plant Physiol. 151, 379.

Stirbet, A., Strasser, B.J., Strasser, R.J., 1998. Chlorophyll a fluorescence induction in

higher plants: modelling and numerical simulation. J. Theor. Biol. 193, 131–151.
Tong, S., Hutchins, D.A., Fu, F., Gao, K., 2016. Effects of varying growth irradiance and nitrogen sources on calcification and physiological performance of the coccolithophore *Gephyrocapsa oceanica* grown under nitrogen limitation. Limnol. Oceanogr. 61, 2234–2242.
Tong, S., Hutchins, D.A., Gao, K., 2019. Physiological and biochemical responses of *Emiliania huxleyi* to ocean acidification and warming are modulated by UV radiation. Biogeoscience 16, 561–572.
Trimborn, S., Longer, G., Rost, B., 2007. Effect of varying calcium concentrations and light intensities on calcification and photosynthesis in *Emiliania huxleyi*. Limnol. Oceanogr. 52, 2285–2293.
Van De Poll, W.H., Eggert, A., Buma, A.G., Breeman, A.M., 2001. Effects of UV-B-induced DNA damage and photoinhibition on growth of temperate marine red macrophytes: habitat-related differences in UV-B tolerance. J. Phycol. 37, 30–38.
Watabe, N., Wilbur, K.M., 1966. Effects of temperature on growth, calcification, and coccolith form in *Coccolithus huxleyi* (Coccolithineae). Limnol. Oceanogr. 11, 567–575.
Xu, K., Gao, K., 2015. Solar UV irradiances modulate effects of ocean acidification on the coccolithophorid *Emiliania huxleyi*. Photochem. Photobiol. 91, 92–101.
Xu, K., Fu, F., Hutchins, D., 2014. Comparative responses of two dominant Antarctic phytoplankton taxa to interactions between ocean acidification, warming, irradiance, and iron availability. Limnol. Oceanogr. 59, 1919–1931.
Zhang, Y., Klapper, R., Lohbeck, K.T., Bach, L.T., Schulz, K.G., Reusch, T.B., Riebesell, U., 2014. Between-and within-population variations in thermal reaction norms of the coccolithophore *Emiliania huxleyi*. Limnol. Oceanogr. 59, 1570–1580.
Zhang, Y., Bach, L.T., Schulz, K.G., Riebesell, U., 2015. The modulating effect of light intensity on the response of the coccolithophore *Gephyrocapsa oceanica* to ocean acidification. Limnol. Oceanogr. 60, 2145–2157.
Zondervan, I., 2007. The effects of light, macronutrients, trace metals and CO_2 on the production of calcium carbonate and organic carbon in coccolithophores-a review. Deep Sea Research Part II 54, 521–537.
Zondervan, I., Rost, B., Riebesell, U., 2002. Effect of CO_2 concentration on the PIC/POC ratio in the coccolithophore *Emiliania huxleyi* grown under light-limiting conditions and different daylengths. J. Exp. Mar. Biol. Ecol. 272, 55–70.